

From Photometric-Motion to Shape from Shading

José R.A. Torreão^{1,2}

¹Pós-Graduação em Informática Aplicada
Pontifícia Universidade Católica do Paraná
80215-901 Curitiba PR, BRAZIL
jrat@ic.uff.br

João L. Fernandes

²Instituto de Computação
Universidade Federal Fluminense
24210-240 Niterói RJ, BRAZIL
ccmjlf@vm.uff.br

Abstract

A new approach to shape estimation from shading input has been recently introduced through the processes of disparity-based photometric stereo (DBPS) and Green's function shape from shading (GSFS). Both processes start from a pair of constraints - a matching constraint and a photometric constraint - to arrive at a closed-form expression for the depth function of the imaged surface. In DBPS, the matching equation is solved for the disparity map, given a pair of photometric stereo images, while in GSFS, which extends the previous approach to single-input reconstruction, that equation is solved for the matching image, via Green's function. Adopting a similar framework, we have recently used photometric and matching constraints for deriving a new approach to the photometric-motion shape estimation problem. Here we show how we can extend that process to the single-input case, via Green's function. This yields high quality shape-from-shading estimates, even from real input obtained under complex illumination.

1. Introduction

Shape estimation from shading input has traditionally been based solely on the photometric aspects of image formation, expressed through the reflectance map function [1, 2]. The reflectance map relates the irradiance at each image point to the gradient at the corresponding location in the scene, via the image irradiance equation,

$$I(x, y) = R(p, q) \quad (1)$$

where

$$p = \frac{\partial Z}{\partial x}, \text{ and } q = \frac{\partial Z}{\partial y} \quad (2)$$

are the surface gradient components, and R is the reflectance map.

Recently, a new framework has been introduced which incorporates more geometry into the monocular reflectance-map based shape estimation processes (shape from shading and photometric stereo), by also making use of image matching information. This approach was pioneered with the disparity-based photometric stereo (DBPS) [3], and later extended with the Green's function shape from shading (GSFS) [4].

In DBPS, given a pair of photometric stereo images (monocular images captured under different illuminations), a linear irradiance equation is assumed for the difference image,

$$\Delta I \equiv I_1 - I_2 = k_0 + k_1 p + k_2 q \quad (3)$$

and a linearized matching equation is also introduced,

$$\Delta I = u \frac{\partial I_2}{\partial x} + v \frac{\partial I_2}{\partial y} \quad (4)$$

to yield the optical flow field, (u, v) .

Equating (3) and (4), there results a differential equation for the surface function $Z(x, y)$, whose solution can be found if the matching is performed along a direction determined by the linear reflectance map components, namely, if $v/u = k_2/k_1 \equiv \gamma$.

Under similar conditions, this approach can be extended to single-input shape estimation, through the Green's function shape from shading, provided that the matching equation $I_2(x + u) = I_1(x)$ is solved for the equivalent to the second photometric stereo image. Taken up to second order in u , such equation becomes

$$\frac{u^2}{2} \frac{\partial^2 I_2}{\partial x^2} + u \frac{\partial I_2}{\partial x} + I_2 = I_1 \quad (5)$$

and, assuming uniform u , I_2 can be found as

$$I_2(x, y + \gamma x) = \int_{\mathcal{D}} G_u(x - x') I_1(x', y + \gamma x') dx' \quad (6)$$

where \mathcal{D} is the image domain. The function $G_u(x - x')$, called the Green's function, is a solution to (5) when an impulse function is substituted for its right-hand side, and can

be given as

$$G_u(x - x') = \begin{cases} \frac{2}{u} \sin\left(\frac{x-x'}{u}\right) e^{-\left(\frac{x-x'}{u}\right)} & x > x' \\ 0 & x < x' \end{cases} \quad (7)$$

Once I_2 is obtained through (6), and assuming a linear irradiance equation for I_1 , shape estimation proceeds in GSFS along similar lines as in DBPS.

Here we will show that the Green's function procedure which allowed us to go from photometric stereo to shape from shading (i.e., from two-image to single-image shape estimation) can also be followed starting from a photometric motion process.

Photometric motion was introduced by Pentland [5], based on his observation that, for surfaces under rotation relative to the camera, the photometric effects of motion - i.e., the intensity change of a moving point - could dominate the purely geometric effects, due to projective distortion. In his formulation, Pentland considered a quadratic Taylor series expansion of the reflectance map, supposed symmetric and separable. He also assumed that regions of approximately linear motion could be identified, allowing the registration of points, in successive frames, which corresponded to the same position on the moving surface. Under such conditions, Pentland found that the intensity difference of the registered points was associated to a linear reflectance map, and he thus employed his linear shape from shading algorithm [6], for shape estimation in the Fourier domain.

Recently, we have introduced an alternative formulation for photometric motion [7], a distinctive feature of which is that of being based on the intensity change, due to the motion, at a fixed location in the image plane, and not, as in the original formulation, at a given point on the moving surface. Here we show how such approach can be extended to single-input reconstruction, also via Green's function, thus leading to better surface estimates than with GSFS.

2. Photometric Motion

Here we review the photometric motion formulation introduced in [7]. Let us consider a surface $Z(x, y)$, rotating about the x and y axes of a static reference frame, and imaged under orthographic projection. The surface motion gives rise to an optical flow, which we will assume identical to the motion field $\mathbf{u} = (u, v)$, for

$$u = \frac{dx}{dt} = BZ, \quad \text{and} \quad v = \frac{dy}{dt} = -AZ \quad (8)$$

where A and B are the angular velocity components along the x and y directions, respectively. From the motion equations, we also get

$$\frac{dZ}{dt} \equiv \frac{\partial Z}{\partial t} + \frac{\partial Z}{\partial x} \frac{dx}{dt} + \frac{\partial Z}{\partial y} \frac{dy}{dt} = Ay - Bx \quad (9)$$

and, from the above,

$$\frac{\partial Z}{\partial t} = -B[Z(p + \gamma q) + (x + \gamma y)] \quad (10)$$

where p and q are the surface gradient components, as in (2), and where we have defined

$$\gamma = -\frac{A}{B} \equiv \frac{v}{u} \quad (11)$$

Equation (11) implies that, for a uniform rotation, the motion field is one-dimensional, the optical flow thus reducing to a disparity map.

Now, let us assume that the image irradiance can be expressed, in terms of surface gradient, through the linear form

$$I = k_0 + k_1 p + k_2 q \equiv k_0 + k_1(p + \gamma q) \quad (12)$$

where $k_2/k_1 = \gamma$, for the same γ as introduced in (11). This means that the surface is assumed to be rotating about an axis perpendicular to the projection of the "generalized illuminant" - i.e., (k_1, k_2, k_0) [6] - over the xy -plane.

The irradiance change due to the motion, at any given image point, can be expressed as

$$\Delta I \equiv I(t - \delta t) - I(t) = -\frac{\partial I}{\partial t} \delta t \quad (13)$$

where δt is the time discretization factor, which will be assumed equal to 1. Using (12) and (10), we thus get

$$\frac{\Delta I}{k_1} = -\frac{\partial(p + \gamma q)}{\partial t} \equiv -\left(\frac{\partial}{\partial x} + \gamma \frac{\partial}{\partial y}\right) \frac{\partial Z}{\partial t} \quad (14)$$

and

$$\frac{\Delta I}{k_1} = \partial_\gamma \{B[Z(p + \gamma q) + (x + \gamma y)]\} \quad (15)$$

where we have defined

$$\partial_\gamma \equiv \frac{\partial}{\partial x} + \gamma \frac{\partial}{\partial y} \quad (16)$$

Again using (12), there results

$$\Delta I = \partial_\gamma \{B[Z(I - k_0) + k_1(x + \gamma y)]\} \quad (17)$$

and substituting $B = u/Z$, from equation (8), we finally arrive at

$$\Delta I = \partial_\gamma \left[u(I - k_0) + \frac{k_1 u}{Z}(x + \gamma y) \right] \quad (18)$$

Equation (18) relates the shape of the imaged surface to its observables: the image sequence and the optical flow. To obtain from it an estimate of the surface function, we now introduce, in the spirit of DBPS, the appropriate matching equation. We choose it as the affine optical flow relation

$$\Delta I = \left[u - (\partial_\gamma u) \left(\frac{x + \gamma y}{1 + \gamma^2} \right) \right] \partial_\gamma I \quad (19)$$

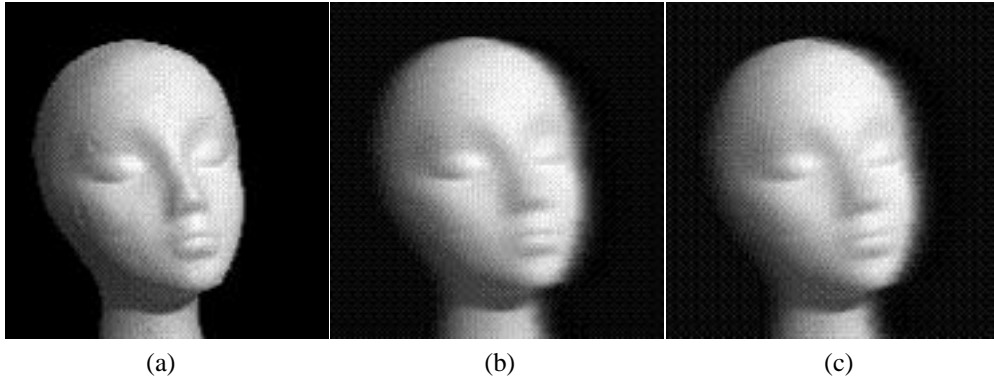


Figure 1. Mannequin image (a), and the result of filtering it, according to (26), along the horizontal direction (b), and along a direction $+10^\circ$ from the horizontal (c) (i.e., for $\gamma = 0$ and $\gamma = 0.175$, respectively). Images (b) and (c) are approximate renditions of the same surface as in (a), but rotated, respectively, about the vertical, and about the axis of the mannequin's nose (Green's function parameters: $a = 2$ and $\sigma = 0.2$, in both cases).

which has the expected form for such one-dimensional matching, as can be seen by recasting it as

$$\Delta I = [|\mathbf{u}| - (\mathbf{x} \cdot \mathbf{s})(\nabla|\mathbf{u}| \cdot \mathbf{s})] \nabla I \cdot \mathbf{s} \quad (20)$$

where $\mathbf{x} = (x, y)$, and $|\mathbf{u}|$ is the magnitude of the disparity vector $\mathbf{u} = u(1, \gamma)$, which points along the matching direction $\mathbf{s} = (\cos \theta, \sin \theta)$, for $\tan \theta = \gamma$.

Equating (18) and (19), we get a differential equation for Z , a solution to which is given by

$$Z(x, y) = -\frac{k_1(1 + \gamma^2)u}{(\partial_\gamma u)(I - k_0)} \quad (21)$$

as can easily be verified by direct substitution, provided the term in $\partial_\gamma^2 u$ is neglected. It is also easy to see that the same result would obtain if the reflectance map coefficients, k_0 and k_1 , varied as functions of $(y - \gamma x)$.

Once successive images of the rotating surface are matched according to (19), equation (21) can be used for recovering the surface function Z from the u and $\partial_\gamma u$ estimates, as discussed in [7]. Here we will show how the same approach can be extended to the single-input case, in what will be called the Green's function photometric motion (GPM).

3. Single-Image Approach

The single-image version of our photometric motion approach is based on the introduction of a Green's function

which relates the matching image to the input image according to equation (20). Since that is a one-dimensional expression, we may, without loss of generality, denote the matching direction by x . We thus require our images to be related as

$$\Delta I \equiv I_1 - I_2 = (u_0 - u_1 x) \frac{\partial I_2}{\partial x} \quad (22)$$

where I_1 is the input image, I_2 is the image derived from it through the Green's function, and u_0 and u_1 are constants associated, respectively, with the disparity map and its derivative.

We propose our Green's function as the Gabor-like form

$$G(x, x') = \frac{2a}{\sigma^2} \sin \left[\frac{a(x - x')}{\sigma^2} \right] e^{-\left[\frac{(x+a)^2 - (x'+a)^2}{2\sigma^2} \right]} \quad (23)$$

for $x > x'$, with $G = 0$ for $x < x'$. When $x, x' \ll a$, G tends to the G_u of equation (7), for $u = \sigma^2/a$, but it is not translation invariant, neither normalized. Denoting by $Int(x)$ its integral over all x' , we can define its normalized version as

$$g(x, x') = \frac{G(x, x')}{Int(x)} \quad (24)$$

where, for small values of σ^2/a ,

$$Int(x) \approx \frac{2a^2}{(x+a)^2 + a^2} \quad (25)$$

which tends to 1 for $x \ll a$.

Given the input image $I_1(x)$, we generate its matching pair through

$$I_2(x) = \int_{\mathcal{D}} g(x, x') I_1(x') dx' \quad (26)$$

The relation between I_1 and I_2 can then be easily obtained as

$$I_1 = \frac{1}{2} \left(\frac{\sigma^2}{a} \right)^2 Int I_2'' + \left[2 \left(\frac{\sigma^2}{a} \right)^2 Int' + \left(\frac{\sigma^2}{a} + x \frac{\sigma^2}{a^2} \right) Int \right] I_2' + I_2 \quad (27)$$

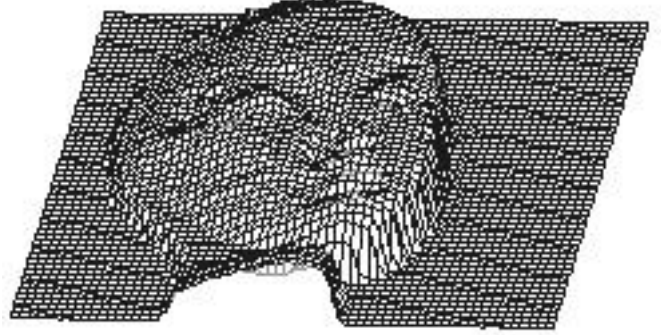
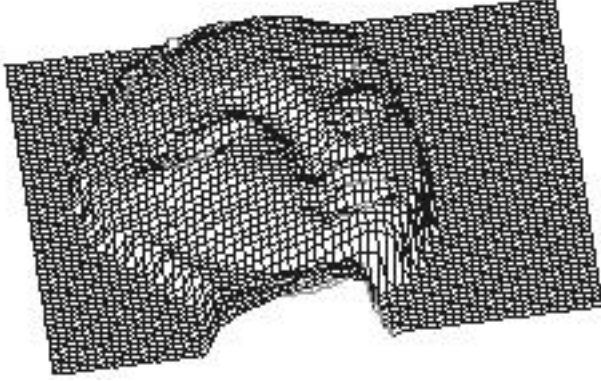
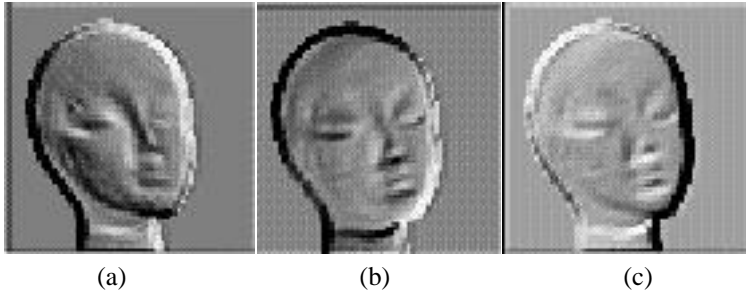


Figure 2. Estimation from mannequin image. (a) to (c): Renditions of the estimated surface function in (d), with lambertian reflectance map and uniform albedo, for illumination from (1,1,1), (1,-1,1), and (-1,1,1); (d) Surface function estimated from Fig. 1(a) through the GPM approach ($\gamma = 0.175$, $a = 2$, $\sigma = 0.1$).

and, to first order in σ^2/a and for $|x| \ll a$, becomes

$$\Delta I = \left(\frac{\sigma^2}{a} + x \frac{\sigma^2}{a^2} \right) I_2' \quad (28)$$

where the primes denote differentiation with respect to x .

Comparing (28) to (22), we see that the proposed Green's function leads to the required matching relation, for

$$u_0 = \frac{\sigma^2}{a} \quad \text{and} \quad u_1 = -\frac{\sigma^2}{a^2} \quad (29)$$

Figure 1 presents an input image and its transformation according to equation (26), for $\gamma = 0$ and $\gamma = 0.175$. It shows that the filter $g(x, x')$ has an effect consistent with our goal of emulating rotations in the scene. Figure 2 presents the 3D reconstruction of the imaged surface, as discussed in the following section.

Before we present our experiments, we should remark that the form I_2 in equation (26) is not the only one to satisfy the required matching condition: other matching im-

(d)

ages result from the linear combination of I_2 with a solution to the homogeneous form of equation (27). Such a solution can be obtained by filtering the input image by a form $H(x, x')$ similar to $G(x, x')$, but with a cosine substituted for the sine function in equation (23). G and H display the following significant property: when filtering certain Gabor-function modulated signals, such as model the response of the simple cells of the visual cortex [8], they yield similar outputs, but for spatially shifted versions of the input signal. This can be proven thus: using the complex representation (and for $x > x'$)

$$(H + iG)(x, x') \equiv 2k e^{ik(x-x')} e^{-\left[\frac{(x+a)^2 - (x'+a)^2}{2\sigma^2} \right]} \quad (30)$$

where $k \equiv a/\sigma^2$, we have for the filtered signal

$$I_2(x) \equiv \int_{\mathcal{D}} (H + iG)(x, x') I_1(x') dx' \quad (31)$$

where

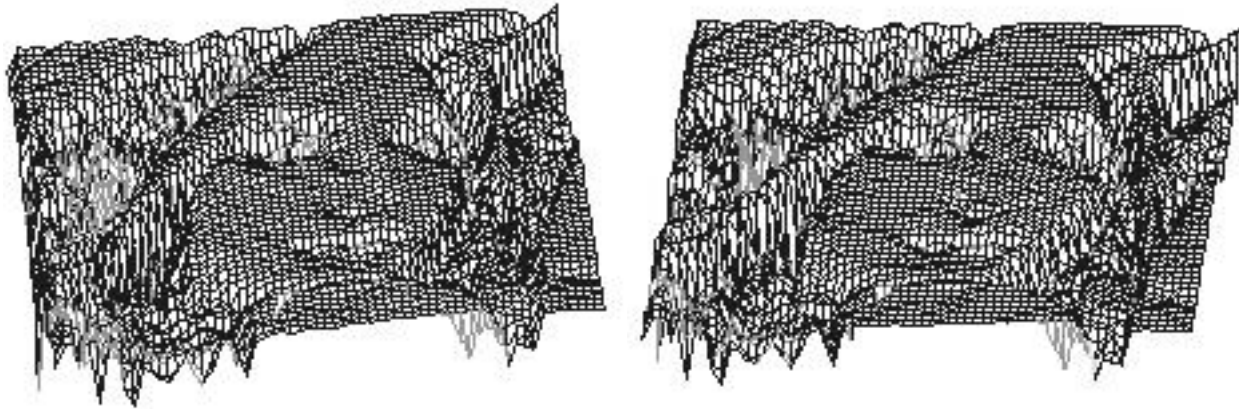
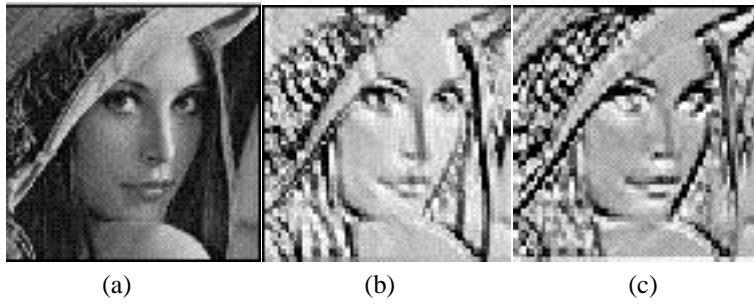
$$I_1(x) = e^{i\kappa x} e^{-\left[\frac{(x+\alpha)^2}{2\sigma^2} \right]} I(x) \quad (32)$$

After some trivial manipulation, (31) yields

$$I_2(x) = e^{i(\kappa x - \phi)} e^{-\left[\frac{(x+\alpha)^2}{2\sigma^2} \right]} \bar{I}(x) \quad (33)$$

where

$$\bar{I}(x) = 2k \int_{\mathcal{D}} e^{i(a-\alpha)\xi/\sigma^2 - (a-\alpha)\xi/\sigma^2} I(x - \xi) d\xi \quad (34)$$



(d)

and $\phi = (\alpha - \kappa\sigma^2)/(\alpha - a)$. As can be verified (compare with (5) and (6)), we have $\bar{I}(x) \equiv I(x - u)$, for $u = \sigma^2/(a - \alpha)$. Such result means that $H + iG$ provides a link between the kind of left- and right-eye signals that are inputs to the disparity-detecting complex cells of the visual cortex. Moreover, such link is exactly as predicted by the so-called phase-difference model of disparity encoding [9], a feature that lends biological plausibility to our shape estimation approach.

4. Experiments

The initial step of the GPM shape estimation procedure is the definition of the matching direction parameter γ , and of the Green's functions parameters, σ and a . Then, given the input image I_1 , its matching pair, I_2 , is obtained by taking the integral in (26), along the chosen direction, over the domain $|x'| \ll a$, such that the approximation in (28) holds. Since the matching relation (26) is one-dimensional, σ and a - and thus also u_0 and u_1 - can, in the general case, be assumed to vary perpendicularly to the matching direction, i.e., as functions of $(y - \gamma x)$, although we have here considered them as uniform. The disparity field and its differential, u and $\partial_\gamma u$, have thus been chosen, consistently with our approximations, as

$$u = u_0 + \left(\frac{x + \gamma y}{1 + \gamma^2} \right) u_1, \text{ and } \partial_\gamma u = u_1 \quad (35)$$

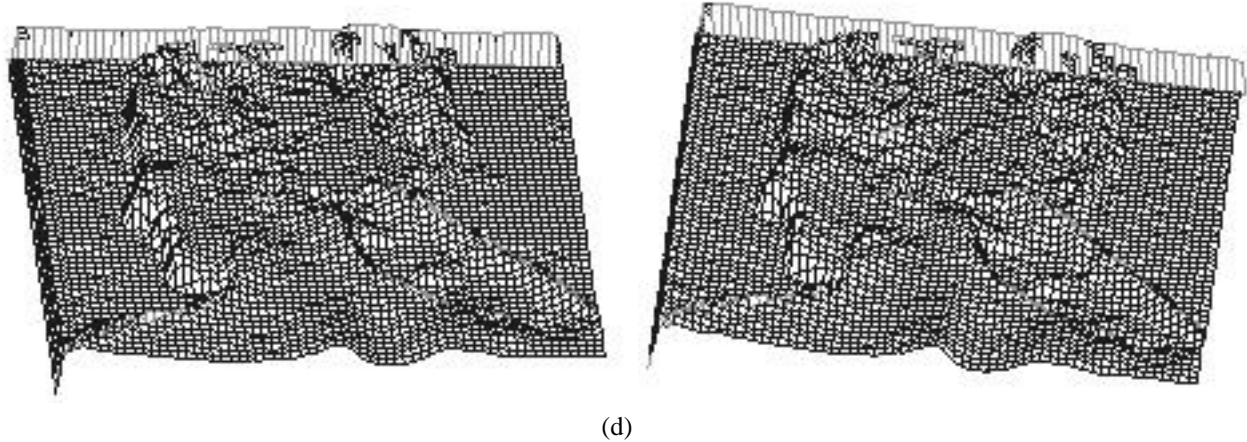
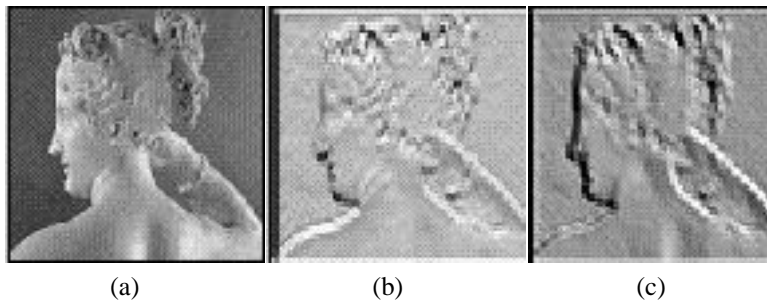
Figure 3. (a) Lenna image; (b) and (c): Renditions of the estimated surface function in (d), with lambertian reflectance map and uniform albedo, for illumination from (0.5,0.5,1) and (0,1,1). GPM parameters: $\gamma = 0$, $a = 2$, $\sigma = 0.1$.

and, from the above, the function $Z(x, y)$ was estimated through equation (21), with I_2 playing the role of I .

Since the reflectance map parameters, k_0 and k_1 , are usually not known, the reconstructions presented here were performed up to the multiplicative factor k_1 , and with k_0 empirically chosen (if the generalized illuminant vector was estimated, such as in [6], this would also inform us the matching direction parameter, $\gamma \equiv k_2/k_1$). Even under such limitations, we have been able to obtain shape estimates of remarkable quality, as shown by the examples of Figures 2 to 4. The reconstruction from the Paolina image of Fig. 4 is particularly noteworthy, due to the complex scene illumination.

5. Summary and Conclusions

Starting from a recently introduced formulation for photometric-motion shape estimation, applicable for surfaces under uniform rotation about the x and y directions [7], we have extended this process to single-input,



(d)

shape-from-shading estimation, in what has been called the Green's function photometric motion (GPM).

Theoretically, under similar assumptions, the multiple-image reconstruction considered in [7] is bound to yield poorer shape estimates than the single-input GPM version here introduced. This is because, by means of the Green's function, in GPM we generate a perfect match to the input image, under the affine condition of equation (19). If we use a real motion pair instead, we first have to solve the tricky optical flow problem of trying to obtain uniform estimates, u_0 and u_1 , such that equation (19) is satisfied. No matter how the real image of the rotated surface looked, or what matching algorithm we used, we can expect no better solution than what would result from matching a single input to its artificial pair, generated as above (incidentally, a similar conclusion has been reached regarding the results of the Green's function shape-from-shading and those of the disparity-based photometric stereo, the former always showing higher quality). Such expectation has been confirmed by our experiments, which have consistently yielded better results than those afforded by the multiple-input algorithm of [7].

The reconstructions obtained via GPM are also far superior to those yielded by its forerunner, the Green's function shape from shading (see [4]), and, judging by the results presented in a recent survey of shape from shading algorithms [1], may be deemed among the best ever, at least for the Lenna image. One reason why GPM outperforms GSFS is because their shared assumption of one-dimensional op-

Figure 4. (a) Paolina image; (b) and (c): Renditions of the estimated surface function in (d), with lambertian reflectance map and uniform albedo, for illumination from (0,1,1) and (1,1,1). GPM parameters: $\gamma = -1$, $a = 2$, $\sigma = 0.1$.

tical flow holds for the former, as proven by equation (11), but only approximately for the latter, as proven in [10].

As described in [11], the Green's functions considered here also find application in edge detection. It is interesting to remark that a possible role for edge-detector cells in SFS estimation has already been suggested by the computer simulation work in [12].

References

- [1] R. Zhang, P.-S. Tsai, J.E. Cryer, M. Shah, Shape from shading: A survey, *IEEE Trans. PAMI* 21(8) (1999) 690-706
- [2] R.J. Woodham, Photometric method for determining surface orientation from multiple images, *Optical Engineering* 19 (1) (1980) 139-144
- [3] J.R.A. Torreão, J.L. Fernandes, Matching photometric stereo images, *Journal of the Optical Society of America A* 15(12)(1998) 2966-2975
- [4] J.R.A. Torreão, A Green's function approach to shape from shading, *Pattern Recognition* 34 (2001) 2367-2382
- [5] A. Pentland, Photometric motion, *IEEE Trans. PAMI* 13(9) (1991) 879-890

- [6] A.P. Pentland, Linear shape from shading, *International Journal of Computer Vision* 4 (1990) 153-162
- [7] J.R.A. Torreão, J.L. Fernandes, H.C.G. Leitão, A novel photometric motion approach, *Proceedings of Sibgrapi 2003*, pp. 294-298, IEEE Computer Society, October 2003
- [8] S. Marcelja, Mathematical description of the responses of simple cortical cells, *Journal of the Optical Society of America* 70 (1980) 1297-1300
- [9] I. Ohzawa, G.C. DeAngelis, R.D. Freeman, Stereoscopic depth discrimination in the visual cortex: neurons ideally suited as disparity detectors, *Science* 249 (1990) 1037-1041
- [10] J.R.A. Torreão, Geometric-photometric approach to monocular shape estimation, *Image and Vision Computing* 21 (2003) 1045-1061
- [11] J.R.A. Torreão, M.S. Amaral, Signal differentiation through a Green's function approach, *Pattern Recognition Letters* 23(4) (2002) 1755-1759
- [12] S.R. Lehky, T.J. Sejnowski, Network model of shape-from-shading: neural function arises from both receptive and projective fields, *Nature* 333 (1988) 452-454